

## Narrow-Band Coherent Anti-Stokes Raman Signals from Broad-Band Pulses

Dan Oron, Nirit Dudovich, Dvir Yelin, and Yaron Silberberg

*Department of Physics of Complex Systems, Weizmann Institute of Science, Rehovot 76100, Israel*

(Received 6 September 2001; published 28 January 2002)

By tailoring the phase of a 100 femtosecond probe pulse we are able to obtain a narrow-band coherent anti-Stokes Raman spectroscopy (CARS) resonant signal with a width of less than  $15 \text{ cm}^{-1}$ , which is an order of magnitude narrower than the CARS signal from a transform limited pulse. Thus, by measuring the spectrum of the CARS signal we are able to obtain a high-resolution energy level diagram of the probed sample in spite of the broad femtosecond pulse spectrum.

DOI: 10.1103/PhysRevLett.88.063004

PACS numbers: 32.80.Qk, 42.65.Dr, 78.47.+p, 82.53.Kp

The concept of quantum coherent control is based on the achievement of constructive interference between different paths of a given system leading to a desirable outcome, while interfering destructively with paths leading to other outcomes. Several works have recently presented coherent control of light interaction with matter, using ultra-short pulses and some form of phase manipulation of the different frequency components of the pulse. Coherent control methods have been applied to stimulated Raman scattering [1,2], two-photon absorption [3,4], control of chemical dissociation [5], and coherent anti-Stokes Raman spectroscopy (CARS) [6]. The various experiments include both ones where the applied phase function is derived theoretically (“open loop”), and adaptive ones [7], where the phase function is determined by a closed feedback loop.

In this work we demonstrate open-loop quantum control of CARS, the most commonly used nonlinear spectroscopic method. In CARS, a pump and a Stokes beam, centered at  $\omega_p$  and  $\omega_s$ , and a probe beam, centered at  $\omega_{pr}$ , illuminate a sample, generating a signal centered at a frequency  $\omega_p - \omega_s + \omega_{pr}$ . The energy level diagram of this process is shown in Fig. 1a. Resonant enhancement of the process occurs when the energy difference  $\omega_p - \omega_s$  coincides with a vibrational level of the medium. Coherent Raman processes have emerged as an important spectroscopic tool in the last few decades [8], especially in the field of femtosecond time-resolved spectroscopy. CARS has recently become a favorable method for nonlinear depth-resolved microscopy [9–12]. The femtosecond

CARS method, however, suffers from a lack of selectivity between neighboring energy levels due to the large bandwidth of the pulses. An increase of the spectral resolution can be achieved either by the use of narrow-band picosecond excitation pulses [12], or by quantum coherent control methods [6]. The latter is the only option in attempting to achieve high-resolution impulsive CARS.

In a complementary publication [6] we demonstrated measurement of high-resolution Raman spectra with femtosecond pulses by selective excitation of the vibrational levels. By shaping both the pump and the Stokes beams it was possible to excite only one of several levels within the pulses bandwidth. In this Letter we present a different mechanism to achieve a similar goal. In contrast to [6], transform limited pump and Stokes pulses are used, so that all levels within the bandwidth of the pump and Stokes beams are excited. We take advantage of the off-resonant polarization to narrow the spectrum of the generated CARS signal from each level by shaping the probe beam. The spectral resolution of the measured Raman spectrum is better than  $15 \text{ cm}^{-1}$ , although the probe beam has a bandwidth of about  $120 \text{ cm}^{-1}$ . The high resolution is demonstrated by differentiating between the two neighboring levels of pyridine having an energy separation of  $40 \text{ cm}^{-1}$ . Enhancement of the CARS signal at a given “target” wavelength by nearly a factor of 2 relative to the maximal signal with a delayed transform limited probe beam is also demonstrated.

The nonlinear polarization driving the CARS signal generated by a three-beam configuration can be approximated by time dependent perturbation theory as

$$P^{(3)}(t) \propto -\frac{1}{\hbar^3} \sum_{mnl} \mu_{gl} \mu_{ln} \mu_{nm} \mu_{mg} \exp[-(i\omega_{lg} + \Gamma_{lg})t] \int_{-\infty}^t dt_1 \int_{-\infty}^{t_1} dt_2 \int_{-\infty}^{t_2} dt_3 \epsilon_p(t_3) \epsilon_s^*(t_2) \epsilon_{pr}(t_1) \times \exp[(i\omega_{ln} + \Gamma_{ln})t_1] \exp[(-i\omega_{mn} + \Gamma_{mn})t_2] \exp[(i\omega_{mg} + \Gamma_{mg})t_3], \quad (1)$$

where  $|m\rangle$ ,  $|n\rangle$ , and  $|l\rangle$  are the intermediate levels,  $\mu_{ij}$  are the dipole moments, and  $\omega_{ij} = (E_i - E_j)/\hbar$ . By assuming that all intermediate levels are far from resonance, we can transform Eq. (1) into the frequency domain, obtaining for nonresonant transitions [3]

$$P_{nr}^{(3)}(\omega) \propto \int_0^\infty d\Omega \epsilon_{pr}(\omega - \Omega) \int_0^\infty d\omega_1 \times \epsilon_s^*(\omega_1 - \Omega) \epsilon_p(\omega_1), \quad (2)$$

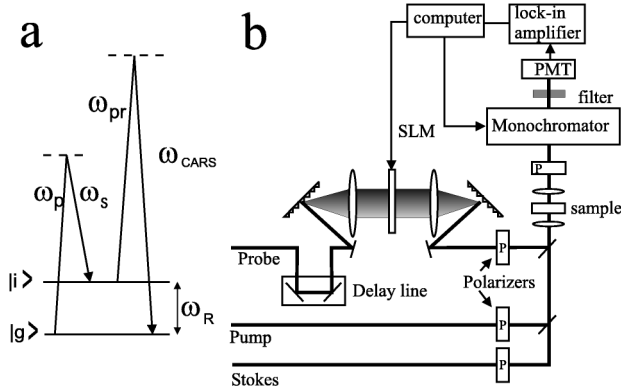


FIG. 1. (a) Energy level diagram of the CARS process. (b) Outline of the experimental setup.

whereas for a singly resonant Raman transition through an intermediate level  $|i\rangle$  at an energy of  $\hbar\omega_R$  and a bandwidth  $\Gamma$  we obtain

$$P_r^{(3)}(\omega) \propto \int_0^\infty d\Omega \frac{\epsilon_{pr}(\omega - \Omega)}{(\omega_R - \Omega) + i\Gamma} \int_0^\infty d\omega_1 \times \epsilon_s^*(\omega_1 - \Omega) \epsilon_p(\omega_1). \quad (3)$$

Phase-only pulse shaping, used in our experiments, simply means multiplication of one or more of the electric fields in Eqs. (2) and (3) by a phase function  $\exp[i\Phi(\omega)]$ . We shall assume that the pump and Stokes are transform limited (unshaped).

As is evident from Eq. (2), the nonresonant signal is maximized by transform limited pulses at zero relative delay for all values of the CARS frequency  $\omega$ , since all the fields  $\epsilon_i(\omega_i)$  are then real and positive.

However, in the resonant case, while the term  $\int_0^\infty d\omega_1 \epsilon_s^*(\omega_1 - \Omega) \epsilon_p(\omega_1)$  is real and positive, the denominator in the  $\frac{\epsilon_{pr}(\omega - \Omega)}{(\omega_R - \Omega) + i\Gamma}$  term inverts phase over a range of width  $\Gamma$  about the resonance frequency  $\omega_R$ . This phase inversion is typical of all driven harmonic systems. Such systems are driven in phase with the driving force below the resonance frequency, in quadrature at the resonance and in opposite phase above it. Hence, when probed with a transform limited field  $\epsilon_{pr}$ , destructive interference is induced between the terms below and above the resonance. To achieve optimal enhancement of the CARS signal at a given frequency  $\omega$ , a spectral phase function  $\Phi = \arctan[(\omega - \omega_R)/\Gamma]$  should be applied on the probe pulse. This enhancement is of a similar nature to that obtained for a two-photon absorption process in atomic Rb vapor by Dudovich *et al.* [4], and to the enhancement of coherent charge oscillations in quantum wells suggested by Weiner [13].

Broadly speaking, the above phase function inverts the relative sign of frequencies much below and above  $\omega - \omega_R$ , and introduces a nearly linear phase for frequencies in a range  $\Gamma$  about  $\omega - \omega_R$ . The linear portion leads to some delay of the pulse. Indeed, it is well known that even for a transform limited probe, a small delay relative to the

pump and Stokes beams results in some enhancement of the entire CARS spectrum.

Ideally, we apply the optimal phase function to maximize the CARS signal at a certain frequency. However, the use of the optimal phase function is limited by the resolution of the pulse shaping apparatus. For levels with a lifetime much larger than the pulse duration, the optimal spectral phase can be approximated by a stepwise inversion of the probe beam phase at a frequency  $\omega - \omega_R$ . When the level linewidth  $\Gamma$  is not negligible compared to the pulse bandwidth, as in the experiments described in the following sections, we found that the peak enhancement can be achieved by application of a smaller ( $<\pi$ ) phase step accompanied by some delay of the probe pulse. A schematic drawing of all these spectral phase functions is plotted in Fig. 2a.

The contribution of the off-resonant polarization components is short-lived in the absence of a driving force. As the detuning from resonance increases, the contribution decreases more rapidly, on a time scale which is much shorter than the level lifetime. Therefore, off-resonant enhancement is a transient effect, lasting only while the shaped probe pulse temporally overlaps the pump and Stokes pulses. As opposed to a simple delay of the probe pulse, the phase step scheme enhances the CARS signal only in a narrow band around  $\omega$ . Thus it is possible to achieve high-resolution spectral measurements even with very broad-band femtosecond pulses.

In our experiments the CARS process involves three exciting pulses: a Ti:sapphire mode locked laser (Spectra

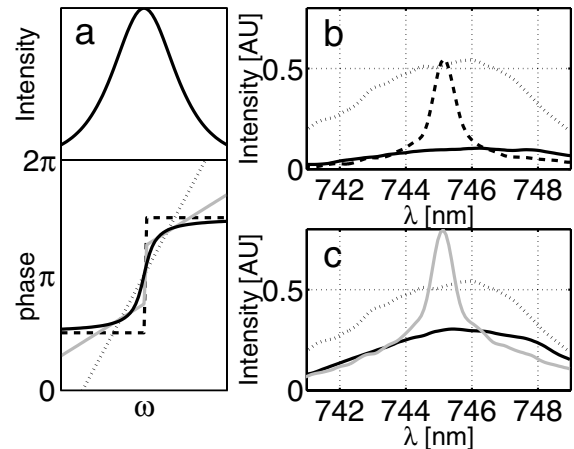


FIG. 2. (a) Schematic drawing of the spectral intensity and various phase functions: optimal phase function (solid line), probe delay (dotted line),  $\pi$  phase step (dashed line),  $\pi/2$  phase step accompanied by some delay (solid gray line). (b) CARS spectrum from a  $\text{Ba}(\text{NO}_3)_2$  sample at zero probe delay for a: transform limited probe (solid line), probe pulse with a  $\pi$  phase step at 808 nm (dashed line), transform limited probe at 300 fs delay (dotted line). (c) CARS spectrum from a  $\text{Ba}(\text{NO}_3)_2$  sample at 100 fs probe delay for a transform limited probe (solid line), probe pulse with a  $\pi/2$  phase step at 808 nm (solid gray line), transform limited probe at 300 fs delay (dotted line).

Physics Tsunami) at 810 nm serving as the probe beam, and both the signal and the idler beams of an optical parametric oscillator (Spectra Physics Opal, pumped by the Ti:sapphire laser) centered at about 1500 and 1760 nm, serving as the pump and Stokes beams, respectively. All beams have a bandwidth of about  $120 \text{ cm}^{-1}$ . The spectral phase of the probe pulses is controlled by Fourier-transform pulse shaping [1,3] using a programmable liquid crystal spatial light modulator (SLM) (CRI SLM-128). The spectral resolution, determined by the spot size of a given frequency in the Fourier plane of the SLM, is about  $5 \text{ cm}^{-1}$  (0.3 nm). As mentioned earlier, the pump and Stokes beams remain transform limited. The beams are polarized so as to measure a nonlinear susceptibility term of the form  $|a\chi_{xyxy} - b\chi_{xyxy}|^2$ . By careful adjustment of the beam polarizations, the nonresonant signal can be eliminated [14]. The three beams are spatially and temporally overlapped in a collinear configuration using dichroic beam splitters and two variable delay lines. The overlapped beams are then focused into the sample using a  $\text{NA} = 0.2$  objective. The CARS signal, collected using a similar numerical aperture lens, passes through a polarizer in order to eliminate the nonresonant signal [14]. It is then filtered by a computer-controlled monochromator, and measured with a photomultiplier tube (PMT) and a lock-in amplifier. The monochromator resolution was set to about 0.5 nm (equivalent to about  $8 \text{ cm}^{-1}$  at 750 nm). An outline of the experimental setup is presented in Fig. 1b.

We first demonstrate narrowing of the CARS spectrum using the  $1048 \text{ cm}^{-1}$  line of a  $\text{Ba}(\text{NO}_3)_2$  crystal. In Fig. 2b we plot the CARS spectrum at zero relative delay for two cases: a transform limited probe pulse, and a pulse with a  $\pi$  phase shift at 808 nm. Also plotted is the CARS spectrum for a transform limited probe at 300 fs delay, at which the CARS signal is maximized. In Fig. 2c we plot the CARS spectrum at a probe delay of 100 fs for two cases: a transform limited probe pulse, and a pulse with a  $\pi/2$  phase shift at 808 nm. Again, we also plot the CARS spectrum for a transform limited probe at 300 fs delay. As can be seen, while for the transform limited case the FWHM of the CARS signal is of the order of the probe spectral width (8 nm), for both shaped cases we get a narrow peak with a FWHM of less than 1 nm (about  $12 \text{ cm}^{-1}$ ). Note that this width results from a convolution of several factors: the level bandwidth ( $0.5 \text{ cm}^{-1}$ ), the pulse shaper resolution ( $5 \text{ cm}^{-1}$ ), the monochromator resolution ( $8 \text{ cm}^{-1}$ ), and some uncompensated dispersion in the excitation beams. As can be seen in Fig. 2c, the enhanced signal at this band is higher by almost a factor of 2 than the maximal signal with a transform limited probe pulse. In Fig. 3 we plot the CARS intensity at the 745 nm peak as a function of the probe delay for the three cases: a transform limited probe pulse, a pulse with a  $\pi/2$  phase shift at 808 nm, and a pulse with a  $\pi$  phase shift at 808 nm. Also plotted are predictions of a numerical solution of the integral in Eq. (3) (note that the finite resolution of the pulse shaper

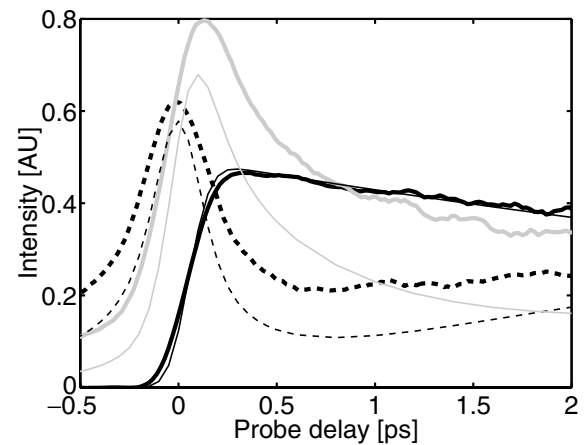


FIG. 3. CARS intensity at 745 nm as a function of the probe delay for three cases: transform limited probe (solid black line), probe pulse with a  $\pi$  phase step at 808 nm (dashed line), and probe pulse with a  $\pi/2$  phase step at 808 nm (solid gray line). Thick lines—experiment; thin lines—model.

is not taken into account). As can be seen, the enhancement of the signal due to the phase step is transient and localized around zero delay.

The ability to differentiate between neighboring Raman levels with an energy spacing much lower than the probe beam bandwidth is demonstrated using the two levels of pyridine, at  $988 \text{ cm}^{-1}$  and at  $1028 \text{ cm}^{-1}$ . Both levels have a similar cross section and a bandwidth of about  $2.2 \text{ cm}^{-1}$ . The CARS spectrum from pyridine at a probe delay of 100 fs is plotted in Fig. 4a for the two cases: a transform limited probe pulse (solid black line), and a pulse with a  $\pi/2$  phase shift at 808 nm (dashed line). The model prediction for the shaped case is also added (solid gray line). Two distinct peaks, related to the two levels of pyridine, are apparent for the shaped case, whereas for the transform limited case a single peak with a FWHM of about 8 nm is obtained. For comparison, we show in Fig. 4b a similar graph of the CARS spectrum of benzene, having a single Raman level at  $992 \text{ cm}^{-1}$ .

Since the CARS signal enhancement is obtained at a frequency corresponding to  $\omega_0 + \omega_R$ , where  $\omega_0$  is the phase step location, we can measure the CARS signal at a given wavelength and scan the phase step location on the SLM rather than visualize the entire spectrum. In Fig. 4c we show the results of such a scan for both pyridine (solid line) and benzene (dashed line). The CARS signal intensity at 748 nm is plotted as a function of the energy difference between the phase step location and the measuring wavelength of 748 nm. Again, two distinct peaks at the corresponding energies are visible in the pyridine spectrum.

In summary, we have demonstrated how, through simple spectral phase manipulation of the probe pulse, we can generate a narrow-band CARS signal from a broad-band probe pulse. The spectral resolution is increased by an order of magnitude. The signal at a given wavelength can be enhanced by almost a factor of 2 relative to the maximal

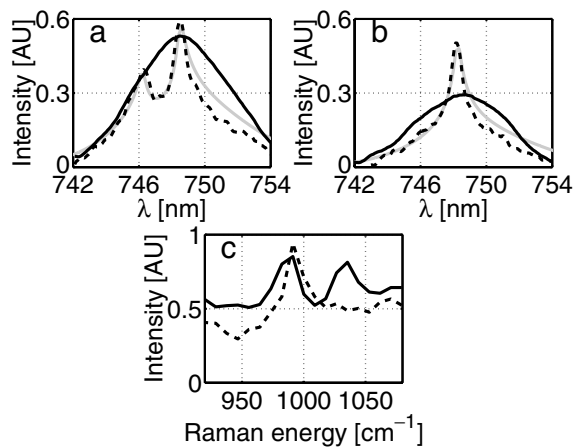


FIG. 4. (a) CARS spectrum from a pyridine sample at 100 fs delay: transform limited probe (solid black line), probe pulse with  $\pi/2$  phase step (dashed line), model prediction for shaped case (solid gray line). (b) Same as (a) for a benzene sample. (c) CARS intensity at 748 nm obtained by scanning the phase step location on the SLM. The energy axis denotes the energy difference between the step wavelength and 748 nm (pyridine—solid line; benzene—dashed line).

signal obtained at this frequency by a transform limited pulse.

Both the spectral resolution and the signal-to-noise ratio achieved by using the shaped probe scheme described in this Letter are similar to those obtained by selective excitation of Raman levels using shaped pump and Stokes pulses [6]. The shaped probe scheme is simpler due to the use of a single shaped beam. It lacks, however, the ability to eliminate the nonresonant signal, as is possible using shaped pump and Stokes beams.

The use of the shaped probe scheme can be particularly attractive for the case of impulsive CARS, when the Raman energy lies within the spectrum of a single ultrashort

pulse. It should be noted that larger enhancement could be achieved using broader excitation and probe pulses, due to the larger value of the off-resonant terms. By use of this scheme it can be possible to obtain high-resolution spectral data otherwise unavailable due to the large spectrum of the impulsive illumination.

Financial support of this research by the Israel Science Foundation and by the German BMBF is gratefully acknowledged.

- 
- [1] A. M. Weiner, D. E. Leaird, G. P. Wiederrecht, and K. A. Nelson, *J. Opt. Soc. Am. B* **8**, 1264 (1991).
  - [2] T. C. Weinacht, J. L. White, and P. H. Bucksbaum, *J. Phys. Chem. A* **103**, 10 166 (1999).
  - [3] D. Meshulach and Y. Silberberg, *Phys. Rev. A* **60**, 1287 (1999).
  - [4] N. Dudovich, B. Dayan, S. M. Gallagher Faeder, and Y. Silberberg, *Phys. Rev. Lett.* **86**, 47 (2000).
  - [5] A. Assion, T. Baumert, M. Bergt, T. Brixner, B. Kiefer, V. Seyfried, M. Strehle, and G. Gerber, *Science* **282**, 919 (1998).
  - [6] D. Oron, N. Dudovich, D. Yelin, and Y. Silberberg, *Phys. Rev. A* (to be published).
  - [7] R. Judson and H. Rabitz, *Phys. Rev. Lett.* **68**, 1500 (1992).
  - [8] *Infrared and Raman Spectroscopy*, edited by B. Schrader (VCH, Weinheim, 1995).
  - [9] A. Zumbusch, G. R. Holtom, and X. S. Xie, *Phys. Rev. Lett.* **82**, 4142 (1999).
  - [10] M. Muller, J. Squier, C. A. de Lange, and G. J. Brakenhoff, *J. Microsc.* **197**, 150 (2000).
  - [11] M. Hashimoto, T. Araki, and S. Kawata, *Opt. Lett.* **25**, 1768 (2000).
  - [12] J. Cheng, A. Volkmer, L. D. Book, and X. S. Xie, *J. Phys. Chem. B* **105**, 1277 (2001).
  - [13] A. M. Weiner, *J. Opt. Soc. Am. B* **11**, 2480 (1994).
  - [14] J. J. Song, G. L. Eesley, and M. D. Levenson, *Appl. Phys. Lett.* **29**, 567 (1976).